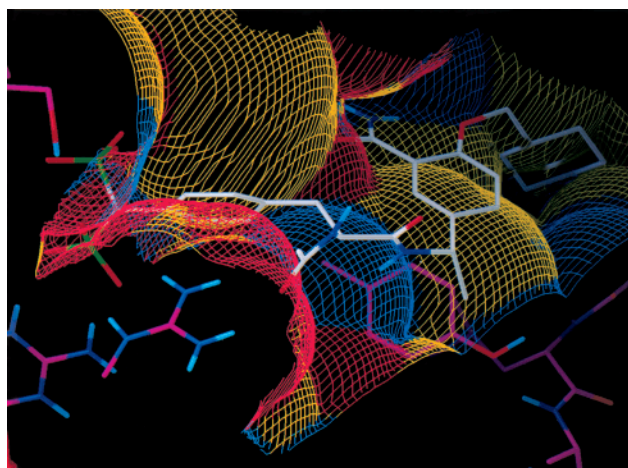


**Figure 1.** (A) Hydrogen bonds formed by phosphotyrosine observed in the X-ray structure of pTyr-Val-Pro-Met-Leu bound to the SH2 domain of Src. Hydrogen bonds are shown with dotted lines. Atoms are colored as follows: oxygen, red; nitrogen, blue; hydrogen, light blue; carbon atoms of the protein, purple; carbon atoms of the ligand, white; phosphorus, green. (B) Hydrogen bonds formed by citrate ion bound to Src SH2 from the Src SH2/citrate X-ray structure. (C) Hydrogen bonds formed by dpmF with Src SH2 predicted by molecular modeling studies.

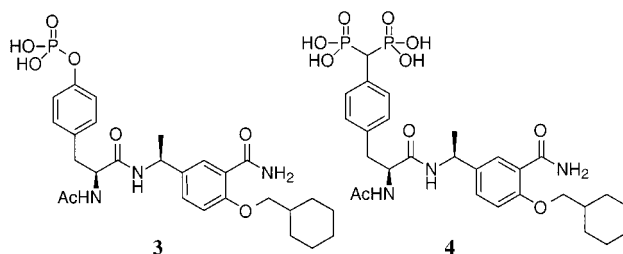
benzamide, as in **3**, can serve as such a linker. Therefore, we modeled molecule **4** which exploits both the dpmF and benzamide/cyclohexyl moieties.

Because the Src SH2/citrate structure contained no ligand atoms in the binding site region beyond the phosphate pocket, this structure was found to be



**Figure 2.** Compound **4** docked into the binding site of Lck SH2. The accessible surface of the binding site is displayed as a mesh, colored to display chemical specificity: hydrophobic regions of the binding site are shown in yellow, hydrogen bond donor regions in red, and hydrogen bond acceptor regions in blue. For optimal van der Waals contact, ligand atoms lie on or close to the mesh. Ligand atoms forming hydrogen bonds with protein atoms penetrate the mesh. Note the oxygen atoms of the dpmF moiety penetrating the mesh as they form hydrogen bonds with atoms of the phosphotyrosine pocket. Generated using the Flo96 software.

unsatisfactory for modeling SH2 ligands. For example, extensive docking studies did not succeed in correctly fitting pYEEI into this binding site. Therefore, we used the high-resolution (1.0 Å) structure of Lck SH2/pYEEI for our modeling studies and conducted conformational searching experiments to simulate the binding of compound **4** to Lck SH2. Figure 2 shows the result of these studies: the dpmF moiety forms the favorable interactions described above; the benzene ring is positioned above Tyr 181 (205 in Src)<sup>13</sup> forming favorable stacking

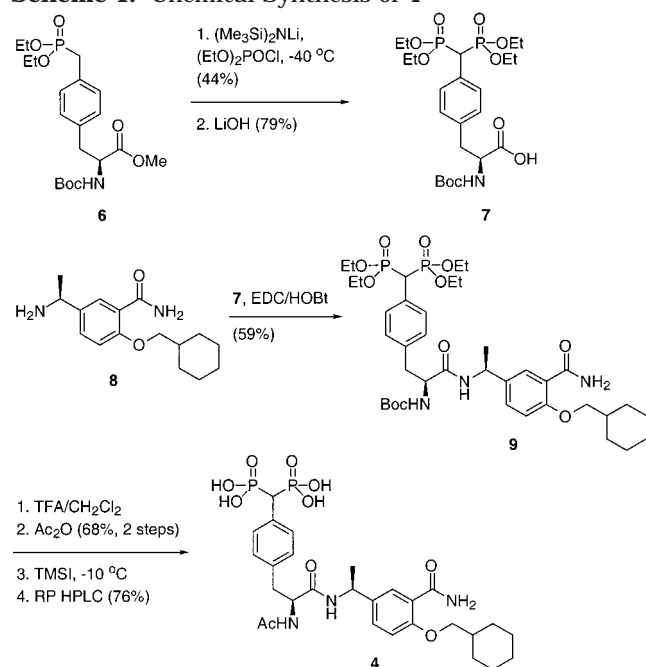


interactions; the benzamide displaces two water molecules forming hydrogen bonds with the backbone NH of Lys 182 (206 in Src) and the backbone carbonyl of Ile 193 (217 in Src); the ether oxygen forms an intramolecular hydrogen bond with the NH of the benzamide enabling the cyclohexyl side chain to form five hydrophobic contacts as it extends into the pY+3 pocket. Because of the additional interactions formed by the second phosphonate of dpmF, we predicted that **4** would bind to Src SH2 with higher affinity than **3**.

Encouraged by these molecular modeling results, we synthesized compound **4**.

**Synthesis.** The synthesis of compound **4** has been optimized as outlined in Scheme 1. (Details of the synthetic procedures are given in the Supporting Information.) For comparison we also synthesized compound **5** (see Table 1).

**Src SH2 Binding Assay.** A fluorescence polarization-based competitive binding assay was used to determine the IC<sub>50</sub> of our compounds to the Src SH2 domain.<sup>14</sup> Results are shown in Table 1.

**Scheme 1. Chemical Synthesis of 4****Table 1. Src SH2 Binding Properties**

Compound	Structure	Src SH2 binding, $\text{IC}_{50}$ , $\mu\text{M}$
Ac-pYEEI-NH <sub>2</sub>		5.0
3		2.2
4		0.35
5		7.9

Comparison of compound **4** with compound **5** shows that the incorporation of the second phosphonate group in the dpmF headgroup resulted in a 22-fold increase in binding affinity. Thus, the combination of the benzamide moiety with this high-affinity pY mimic resulted in a compound with a 14-fold higher binding affinity than that of the cognate peptide.

**Hydroxyapatite Binding.** The presence of the diphosphonomethyl group in **4** suggests that the molecule might target to bone in vivo. The bisphosphonate moiety has been shown to bind to bone and is present in a number of drugs used clinically to treat osteoporosis.<sup>15</sup> To evaluate this in vitro, a bone-binding model was developed. A microcrystalline hydroxyapatite adsorption column with phosphate gradient elution was used to

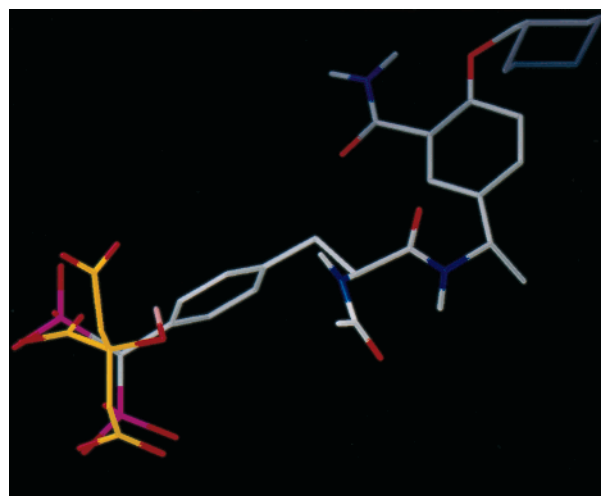


**Figure 3.** Conformation adopted by compound **4** upon binding to Src SH2 predicted by molecular modeling in green, determined by NMR in yellow, and determined by X-ray crystallography in blue. Prepared by superimposition of binding site atoms.

measure the affinity of particular bone-targeting groups to hydroxyapatite. Tighter binding compounds elute later in the gradient. Retention time is expressed in terms in  $K'$ , the number of void volumes required to elute a particular compound.

The hydroxyapatite chromatography results show that neither Ac-pYEEI-NH<sub>2</sub> nor compound **5** have measurable affinity for hydroxyapatite ( $K' < 0.1$ ). On the other hand, compound **4** has a similar affinity for hydroxyapatite ( $K' = 3.7$ ) as alendronate ( $K' = 3.6$ ), a bone-targeted bisphosphonate drug. These results suggest that the diphosphonomethyl moiety of **4** is responsible for its affinity to hydroxyapatite and that **4** will bind to bone with affinity similar as alendronate.

**Rabbit Osteoclast Resorption.** Because Src has been implicated in the regulation of osteoclast functional activity, we tested the ability of compound **4** to inhibit osteoclast-mediated resorption of dentine. Compound **4** inhibited resorption of dentine with an  $\text{IC}_{50}$  of  $2\ \mu\text{M}$ . This is a significant improvement over a recently reported Src-modifying aldehyde compound (with an  $\text{IC}_{50}$  of  $43\ \mu\text{M}$ ), also developed in these laboratories.<sup>4</sup> To rule out the possibility that the observed antiresorptive activity of compound **4** was not due to nonspecific association with the bone matrix, we synthesized an analogue containing the dpmF moiety which possesses no affinity for the Src SH2 domain. This molecule did not demonstrate any antiresorptive activity.

**Structure Determination.** To confirm the predicted binding mode of **4**, the structure of its complex with Src SH2 was determined by NMR and that of its complex with the mutated Lck SH2 (S164C) by X-ray crystallography. The experimentally determined binding conformations of **4** proved to be very similar to those predicted by molecular modeling (Figure 3). NMR experiments revealed 46 NOEs between compound **4** and the protein. These clearly indicate that the dpmF of compound **4** occupies the pY pocket and that the cyclohexyl moiety binds in the pY+3 pocket.

The X-ray structures of the Lck SH2/**4** complex reveals that the dpmF binds, as predicted, with the phenyl ring in a position very similar to that of pY in the pYEEI complex. The benzamide group is stacked against the benzene ring of Tyr 181 (205 in Src). The

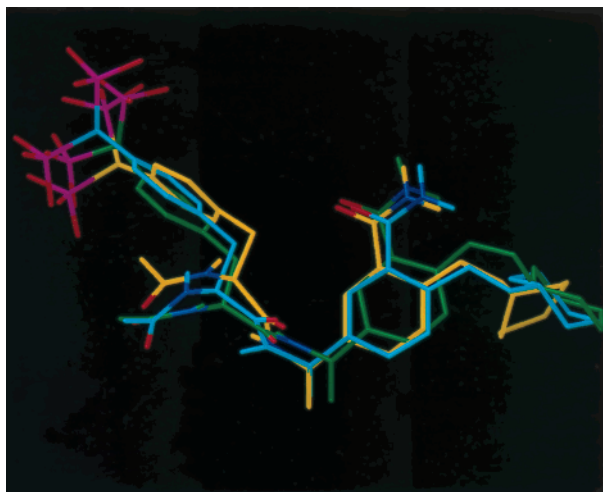


**Figure 4.** Comparison between citrate and compound **4** from the crystal structure of Src SH2/citrate and Lck SH2 (S164C)/**4**, constructed by superimposition of the binding site atoms.

benzamide carbonyl oxygen is in a position occupied by a water molecule in the pYEEI structure and forms a hydrogen bond with the backbone NH of Lys 182 (206 in Src). There are also two water molecules in this vicinity, and the temperature factors of these waters are as low as the backbone chain of Lck SH2, indicating that they are highly localized and held together by a number of strong hydrogen bonds. There are two direct and four water-mediated hydrogen bonds between the benzamide group and the protein. The cyclohexyl group forms extended contacts with the pY+3 pocket although it does not extend as deeply into the pY+3 pocket as the Ile side chain of pYEEI. An unexpected difference between the Lck SH2/**4** structure and that of previous SH2/ligand complexes is the open conformation of the BC loop. However, the crystal structure of a close analogue of compound **4** displays the BC loop in a position similar to that found in the Src SH2/citrate structure, forming hydrogen bonds with the second phosphate as predicted by our model.<sup>16</sup> NMR results also clearly indicate that the BC loop is in contact with the dpmF group of compound **4**. Thus, we conclude that the open loop conformation observed in the X-ray structure is due to crystal packing effects.

Another difference between the predicted ligand-binding mode and the X-ray structure is the presence in the X-ray structure of a water molecule between the NH<sub>2</sub> group of the benzamide and the carbonyl of Ile 193. As no water molecules are present in our binding site model, the NH<sub>2</sub> group of the benzamide was predicted to form a direct, weak hydrogen bond with the carbonyl of Ile 193, instead of the water-mediated hydrogen bond observed in the X-ray structure.

The superposition of complexes of Lck SH2 with compound **4** predicted by molecular modeling and determined by X-ray crystallography are shown in Figure 3. The binding mode of compound **4** determined by NMR has also been superimposed. Figure 4 shows a close-up of the superposition of the X-ray structures of the dpmF moiety from the Lck SH2/**4** complex and the Src SH2/citrate complex.

**Conclusion.** A crystal structure of the citrate ion bound to Src SH2 revealed that the phosphotyrosine pocket of Src SH2 offers hydrogen-bonding opportunities in addition to those displayed by natural pY-containing

ligands. Molecular modeling predicted that a geminal bisphosphonate could form interactions similar to those of citrate. Incorporation of this moiety into a nonpeptidic ligand for Src SH2 resulted in a compound which had 14 times greater binding affinity than the cognate (natural) peptide, possessed bone-binding properties, and inhibited osteoclast-mediated resorption of dentine. X-ray and NMR structures of the compound bound to Src and Lck SH2 agreed with molecular modeling predictions. These findings should provide a new paradigm for the design of agents to treat osteoporosis.

**Supporting Information Available:** Experimental details. This material is available free of charge via the Internet at <http://pubs.acs.org>.

## References

- (1) Lowell, C.; Soriano, P. Knockouts of Src-family kinases: stiff bones, wimpy T-cells and bad memories. *Genes Dev.* **1996**, *10*, 1845–1857.
- (2) Missbach, M.; Jeschke, M.; Feyen, J.; Muller, K.; Glatt, M.; Green, J.; Susa, M. A novel inhibitor of the tyrosine kinase Src suppresses phosphorylation of its major cellular substrates and reduces bone resorption in vitro and in rodent models in vivo. *Bone* **1999**, *24*, 437–439.
- (3) Schwartzberg, P. L.; Xing, L.; Hoggmann, O.; Lowell, C. A.; Garrett, L.; Boyce, B. F.; Varmus, H. E. Rescue of osteoclast function by transgenic expression of kinase-deficient Src in src-/- mutant mice. *Gene Dev.* **1997**, *11*, 2835–2844.
- (4) Violette, S.; Shakespeare, W. C.; Bartlett, C.; Guan, W.; Smith, J. a.; Rickles, R. J.; Bohacek, R. S.; Holt, D. a.; Baron, R.; Sawyer, T. K. A Src SH2 selective binding compound inhibits osteoclast-mediated resorption. *Chem. Biol.* **2000**, *7*.
- (5) Songyang, Z.; Shoelson, S. E.; Chaudhuri, M.; Gish, G.; Pawson, T.; Haser, W. G.; King, F.; Roberts, T.; Ratnofsky, S.; J., L. R.; Neel, B. G.; Birge, R. B.; Fajardo, J. E.; Chou, M. M.; Hanafusa, H.; Schaffhausen, B.; Cantley, L. C. SH2 domains recognize specific phosphopeptide sequences. *Cell* **1993**, *72*, 1–20.
- (6) Tong, L.; Warren, T. C.; King, J.; Betageri, R.; Rose, J.; Jakes, S. Crystal Structures of the human p56Lck SH2 domains in complex with two short phosphotyrosyl peptides at 1.0 Angstroms and 1.8 Angstroms resolution. *J. Mol. Biol.* **1996**, *256*, 601–610.
- (7) Waksman, G.; Kominos, D.; Robertson, S. C.; Pant, N. Crystal Structure of Phosphotyrosine Recognition Domain SH2 of V-Src complexed with Tyrosine-phosphorylated peptides. *Nature* **1992**, *358*, 646.
- (8) Gilmer, T.; Rodriguez, M.; Jordan, S.; Crosby, R.; Allgood, K.; Green, M.; Kimery, M.; Wagner, C.; Kinder, D.; Charifson, P.; Hassell, A. M.; Willard, D.; Shampine, L.; Davis, R.; Robbins, J.; Patel, I. R.; Kassel, D.; Burkhardt, W.; Moyer, M.; Bradshaw, T.; Berman, J. Peptide Inhibitors of src SH3-SH2-Phosphoprotein Interactions. *J. Biol. Chem.* **1994**, *269*, 31711–31719.
- (9) McMartin, C.; Bohacek, R. S. QXP: Powerful, rapid computer algorithms for structure-based drug design. *J. Comput.-Aided Mol. Des.* **1997**, *11*, 333–334.
- (10) *McMartin*; ThistleSoft, Inc.: Colebrook, CT, 06021; e-mail [cmcmc@ix.netcom.com](mailto:cmcmc@ix.netcom.com).
- (11) Lunney, E. A.; Para, K. S.; Plummer, M. S.; Prasad, J. V. N. V.; Saltiel, A. R.; Sawyer, T. K.; Shahripour, A.; Singh, J.; Stankovic, C. J. Patent WO97/12903, 1997.
- (12) Para, K.; Lunney, E. A.; Plummer, M.; Stankovic, C. J.; Shahripour, A.; Holland, D.; Rubin, J. R.; Humblet, C.; Fergus, J.; Marks, J.; Hubbell, S.; Herrera, R.; Saltiel, A. R.; Sawyer, T. K. In *Proceedings of the Fifteenth American Peptide Symposium*; Tam, J., Kaumaya, P., Eds.; Escom Science Publishers: Leiden, The Netherlands, 1999; pp 173–175.
- (13) Protein residue numbers were obtained from Swiss-Prot ([www.expasy.ch](http://www.expasy.ch)) for human Src and human Lck. However, unlike Swiss-Prot, we are taking the initiator Met as residue number 1 rather than residue number 0. Where comparisons between Lck and Src are relevant, residue numbers for Src are given in parentheses.
- (14) Lynch, B. A.; Llocacono, K. A.; Tiong, C. L.; Adams, S. E.; A., M. I. A fluorescence polarization based Src-SH2 binding assay. *Anal. Biochem.* **1997**, *247*, 777–782.
- (15) Geddes, A. D.; D'Souza, S. M.; Ebetino, F. H.; Ibbotson, K. J. Bisphosphonates: Structure-activity relationships and therapeutic implications. *Bone Miner. Res.* **1994**, *8*, 265–306.
- (16) Shakespeare, W.; Bohacek, R. S.; Azimioria, M. D.; Macek, K. J.; Luke, G. P.; Hatada, M. H.; Lu, X.; Violette, S. M.; Bartlett, C.; Sawyer, T. Structure-based design of novel bicyclic nonpeptide inhibitors of the Src SH2 domain. *J. Med. Chem.* **2000**, *43*, 3815–3819.

JM0002681